

# DETECTING POP III OBJECTS WITH NGST

**A. Ferrara**<sup>1,2</sup>, **S. Marri**<sup>3</sup>

<sup>1</sup> Joint Institute for Laboratory Astrophysics, Boulder, USA

<sup>2</sup> Osservatorio Astrofisico di Arcetri, Firenze, Italy

<sup>3</sup> Dipartimento di Astronomia, Università di Firenze, Italy.

## ABSTRACT

We discuss some aspects concerning the formation and the impact of the first luminous structures in the universe (PopIIIs), with particular emphasis on their feedback effects on subsequent galaxy formation. We argue that supernovae in these objects might provide, if detected, important constraints for cosmological models. Some of these constraints come from the gravitational magnification of the supernova flux due to the intervening cosmological matter distribution which results in different predictions, for example, on rates, magnification probability, detection limits and number counts of distant supernovae. We show that NGST can tremendously contribute to such a study due to its advanced technological capabilities.

## 1. POP III OBJECTS

Current models of cosmic structure formation based on CDM scenarios predict that the first collapsed, luminous (PopIIIs) objects should form at redshift  $z \approx 30$  and have a total mass  $M \approx 10^6 M_\odot$  or baryonic mass  $M_b \approx 10^5 M_\odot$  (Couchman & Rees 1986, Haiman et al. 1997, Tegmark et al. 1997). This conclusion

is reached by requiring that the cooling time,  $t_c$ , of the gas is shorter than the Hubble time,  $t_H$ , at the formation epoch. In a plasma of primordial composition the only efficient coolant in the temperature range  $T \leq 10^4$  K, the typical virial temperature of PopIII dark matter halos, is represented by  $H_2$  molecules whose abundance increases from its initial post-recombination relic value to higher values during the halo collapse phase. It is therefore crucial to determine the cosmic evolution of such species in the early universe to clarify if small structures can continue to collapse according to the postulated hierarchical structure growth or if, lacking a cooling source, the mass build-up sequence comes to a temporary halt.

### 1.1 Negative Feedback ?

The appearance of PopIIIs is now thought to cause a partial destruction of the available molecular hydrogen either in the intergalactic medium (IGM) and/or in collapsing structures; the result is a negative feedback on galaxy formation. This effect has been pointed out by HRL, and works as follows. As stars form in the very first generation of objects, the emitted

photons in the energy band 11.2-13.6 eV are able to penetrate the gas and photodissociate  $\text{H}_2$  molecules both in the IGM and in the nearest collapsing structures, if they can propagate that far from their source. This negative feedback and its possible limitations are discussed by Ciardi, Ferrara & Abel (1998). In brief, these authors have studied the evolution of ionization and dissociation spheres produced by and surrounding PopIIIs, which are supposed to have total masses  $M \approx 10^6 M_\odot$  and to turn on their radiation field at a redshift  $z = 30$ . By a detailed numerical modelling of non-equilibrium radiative transfer, they conclude that the typical size of the dissociated region is  $R_d \approx 1 - 5$  kpc. As the mean distance between PopIIIs at  $z \approx 20 - 30$  in a CDM model is  $d \approx 0.01 - 0.1$  Mpc, *i.e.* larger than  $R_d$ . Thus, at high redshift, the photodissociated regions are not large enough to overlap. In the same redshift range, the soft-UV background in the Lyman-Werner bands (photons leading to  $\text{H}_2$  photodissociation) when the intergalactic H and  $\text{H}_2$  opacity is included, is found to be  $J_{LW} \approx 10^{-28} - 10^{-26} \text{ erg cm}^{-2} \text{ s}^{-1} \text{ Hz}^{-1}$ . This value is well below the threshold required for the negative feedback of PopIIIs on the subsequent galaxy formation to be effective before redshift  $\approx 20$ .

### 1.2 Positive Feedback

In addition to the uncertain impact of negative feedback, Ferrara (1998) has suggested that instead PopIIIs might be able to provide a *positive* feedback based on supernova (SN) explosions, which, under many aspects, is reminiscent of a scaled

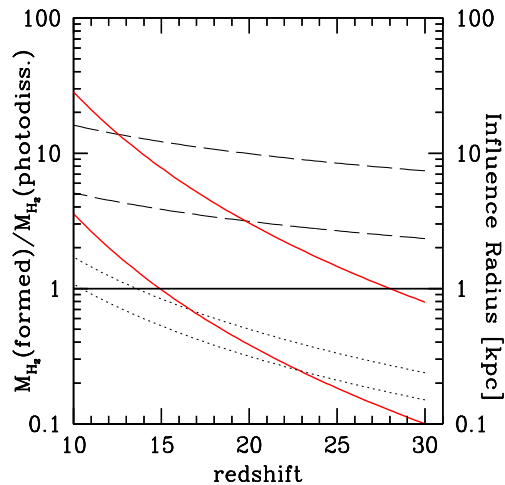


Figure 1: *Ratio between the  $\text{H}_2$  mass formed and destroyed by a PopIII as a function of the multi-SN explosion redshift (solid lines); values larger than one for the ratio define the epochs where PopIIIs have a positive feedback on galaxy formation. Also shown are the shell (proper) radius at cooling,  $R_s(t_c)$  (dotted), and the photodissociation (proper) radius,  $R_d$  (dashed). The upper set of curves refers to objects of mass  $M = 10^6 M_\odot$ , whereas the bottom one corresponds to larger objects,  $M = 10^7 M_\odot$ . The cosmological parameters are  $\Omega_b = 0.05$ ,  $h = 1$ .*

version of the explosive galaxy formation scenario introduced by Ostriker & Cowie (1981) and put forward by many others. PopIIIs are very fragile due to their low mass and shallow gravitational potential: only a few SNe are sufficient to blow-away (Ciardi & Ferrara 1997) their baryonic content and drive an expanding blastwave into the IGM, which eventually becomes radiative and allows the swept gas to cool in a dense shell. Typically a  $H_2$  fraction  $f = 6 \times 10^{-3} f_6$  is formed after explosive events leading to the blow-away of PopIIIs. In order to evaluate the impact of PopIIIs on the subsequent galaxy formation, largely regulated by the availability of  $H_2$  in this mass (and redshift) range, it is useful to compare the  $H_2$  mass production vs. destruction. The ratio between the  $H_2$  mass produced and destroyed by PopIIIs is

$$\frac{M_{H_2}^+(z)}{M_{H_2}^-(z)} = \left( \frac{f}{f_{IGM}} \right) \left[ \frac{R_s(t_c)}{R_d} \right]^3, \quad (1)$$

where  $R_s(t_c)$  is the radius of the SN-driven shell at one gas cooling time. The post-recombination relic fraction of intergalactic  $H_2$  is estimated to be  $f_{IGM} \approx 2 \times 10^{-6} h^{-1}$  (Palla et al. 1995; Anninos & Norman 1996; Lepp, private communication). The previous relation is graphically displayed in Fig. 1, along with the values of  $R_s(t_c)$  and  $R_d$ . From that plot we see that objects of total mass  $M_6 = 1$  produce more  $H_2$  than they destroy for  $z \lesssim 25$ ; larger objects ( $M_6 = 10$ ) provide a similar positive feedback only for  $z \lesssim 15$ , since they are characterized by a higher

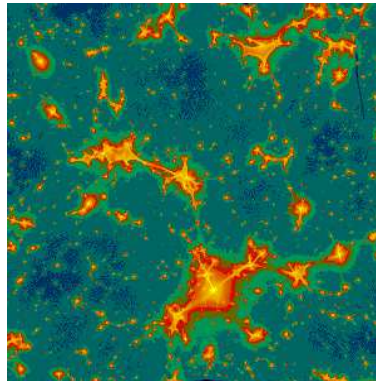


Figure 2: (Color Fig.) Magnification map for the LCDM model at redshift  $z = 8$ ; the strongest caustics (white regions) correspond to magnifications  $\mu \approx 30$ .

$R_d/R_s(t_c)$  ratio. However, since in a hierarchical model larger masses form later, even for these objects the overall effect should be a net  $H_2$  production. This occurrence suggests that these first objects might have a positive feedback on galaxy formation.

## 2. LENSING OF HIGH- $z$ SNe

If PopIIIs can be able to escape destruction of their  $H_2$  molecular content, enough cooling will be available to initiate their gravitational collapse. As the collapse proceeds, the gas density increases and stars are likely to be formed. However, the final product of such star formation activity is presently quite unknown. This uncertainty largely depends on our persisting ignorance on the fragmentation process and its relationship with the thermodynamical

conditions of the gas, both at high  $z$  and, in a less severe manner, in present day galaxies. Ultimately, this prevents firm conclusions on the mass spectrum of the formed stars or their IMF. This problem was already clear more than two decades ago, as pioneering works (Silk 1977; Kashlinsky & Rees 1983; Palla, Salpeter & Stahler 1983; Carr et al. 1984) could not reach similar conclusions on the typical mass range of newly formed stars in the first protogalactic objects. If the IMF is more of the standard type, questions arise about its shape and median value. A common claim in the literature is that the absence of metals (as it is the case in a collapsing PopIII) should shift the peak and the median of the IMF toward higher masses. Obviously, assessing the presence of massive stars that produce ionizing photons and die as Type II supernovae would be of primary importance to clarify the role of PopIIIs in the reionization, photodissociation, and reheating of the universe, and, in general, for galaxy formation. Thus, studying the formation of the first stars has become one of the most challenging problems in physical cosmology. If SNe are allowed to occur at these very high redshifts, they could outshine their host protogalaxy by orders of magnitude and likely become the most distant observable sources since the QSO redshift distribution has an apparent cutoff beyond  $z \approx 4$ . Nevertheless, even for (future) large telescopes as NGST, VLT and Keck this will not be an easy task, this requiring to reach limiting magnitudes  $\approx 32$  in the near IR to observe a SN exploding at  $z = 10$ .

Marri & Ferrara (1998, MF) have investigated the gravitational lensing (GL) magnification effects on high- $z$  SNe in three different cosmological models: SCDM (Standard Cold Dark Matter:  $\Omega_M = 1$ ), LCDM (Lambda Cold Dark Matter:  $\Omega_M = 0.4, \Omega_\Lambda = 0.6$ ), CHDM (Cold Hot Dark Matter:  $\Omega_M = 1, \Omega_\nu = 0.3$ ); all models have  $h = 0.65$ , and are normalized to the present abundance of clusters. The main output of the ray-shooting numerical simulations are a set of magnification maps displaying the magnification,  $\mu$  (*i.e.* the source flux enhancement factor) of a point source located at a given spatial position inside the considered  $4' \times 4'$  field of view. As an example we show in Fig. 2 the magnification map relative to the LCDM model at redshift  $z = 8$ , where the caustics are clearly identified; the maps for all models at different redshifts can be found in MF. There are several unambiguous differences among the three families of cosmological models that we can identify by analysing the magnification maps. SCDM models give intense, but not very numerous caustics ( $\mu \approx 30 - 40$ ) for  $z_s \approx 3$ ; intermediate magnification caustics appear at higher  $z_s$  due to lower mass objects that have not yet hierarchically merged into larger ones. LCDM models produce the most intense caustics ( $\mu \approx 50$ ), but most of the map is covered with more diffuse and lower  $\mu$  magnification patterns. Finally, CHDM models, which form large structures later than  $z = 3$ , show very rare intense events and many moderate  $\mu$  caustics. The magnification probability func-

tion presents a moderate degree of evolution up to  $z \approx 5$  (CHDM) and  $z \approx 7$  (SCDM/LCDM). All models predict that statistically large magnifications,  $\mu \gtrsim 20$  are achievable, with a probability of the order of a fraction of percent, the SCDM model being the most efficient magnifier. All cosmologies predict that above  $z \approx 4$  there is a 10% chance to get magnifications larger than 3.

### 3. NGST EXPECTATIONS

The advances in technology are making available a new generation of instruments, some already at work and some in an advanced design phase, which will dramatically increase our observational capabilities. As representative of such class, we will focus on a particular instrument, namely the Next Generation Space Telescope (NGST). In the following we will try to quantify the expectations for the detection of high  $z$  SNe and the role that the gravitational lensing can play in such a search.

We will assume that NGST (i) is optimized to detect radiation in the wavelength range from  $\lambda_{min} = 1\mu\text{m}$  to  $\lambda_{max} = 5\mu\text{m}$  (*i.e.* J-M bands), and (ii) can observe to a limiting flux of  $\mathcal{F}_{NGST} = 10 \text{ nJy}$  in  $10^2 \text{ s}$  in that range, which should allow for low-resolution spectroscopic follow-up. This can be achieved, for a 8-m (10-m) mirror size and a S/N=5, in about  $2.6 \times 10^4 \text{ s}$  ( $1.1 \times 10^4 \text{ s}$ )<sup>1</sup> We also assume that a Type II SN has a black-body spectrum (Kirshner 1990) with tem-

perature  $T_{SN}$  and we fix its luminosity  $L_{SN} = 3 \times 10^{42}$  (Woosley & Weaver 1986; Patat et al. 1994). This constant luminosity plateau lasts for about  $\approx 80(1+z)$  days, after which the object fades away.

#### 3.1 Apparent Magnitudes

Fig. 3 shows the apparent AB magnitude of a SN as a function of its explosion redshift in four wavelength bands (J, K, L, M) in the assumed NGST sensitivity range, and we compare it with the instrument flux limit. Note that we have taken into account absorption by the IGM at frequencies higher than the hydrogen Ly $\alpha$  line. The plot also assumes that  $T_{SN} = 25000 \text{ K}$ , a value corresponding to the temperature approximately appropriate to the first  $15(1+z)$  days after the explosion (Woosley & Weaver 1986). Including GL magnification enhances dramatically the observational capabilities. In fact, as one can see from the solid line set of curves in Fig. 3, even allowing for a magnification  $\mu = 3$  only, which in all models has a magnification probability larger than 10% at high  $z$ , this pushes the maximum redshift at which SNe can be detected up to  $z \approx 9$

#### 3.2 Detection Limits

A different way to appreciate the GL effects is illustrated by Fig. 4. There we allow for the SN temperature to vary in the large interval  $T_{SN} \approx 4000 - 10^5 \text{ K}$  and we ask in which region of the  $(1+z) - T_{SN}$  parameter space NGST will be able to detect SNe in primordial objects. This region is constrained by the requirement that the radiation from the SN (or the maximum of its black-body spectrum) falls in be-

<sup>1</sup>Result obtained using the NGST Exposure Time Calculator

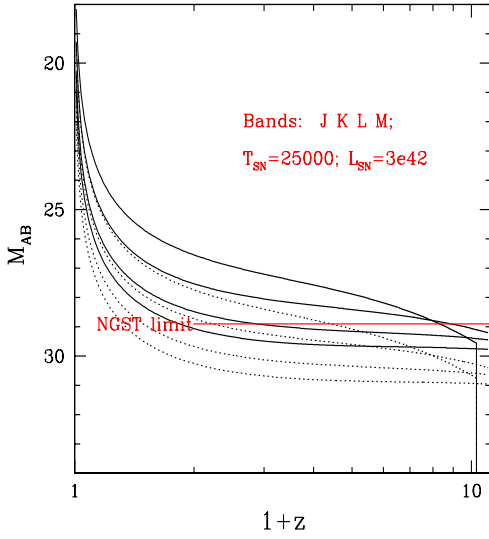


Figure 3: Apparent AB magnitude of a SN as a function of its explosion redshift in the four wavelength bands J, K, L, M (from the uppermost to the lowermost curve) for the SCDM model. The case for a moderate ( $\mu = 3$ ) magnification (solid curves) is compared to the one in which magnification is neglected (dotted). The NGST flux limit is also shown; the vertical line at high redshift in the J band is due to intergalactic absorption.

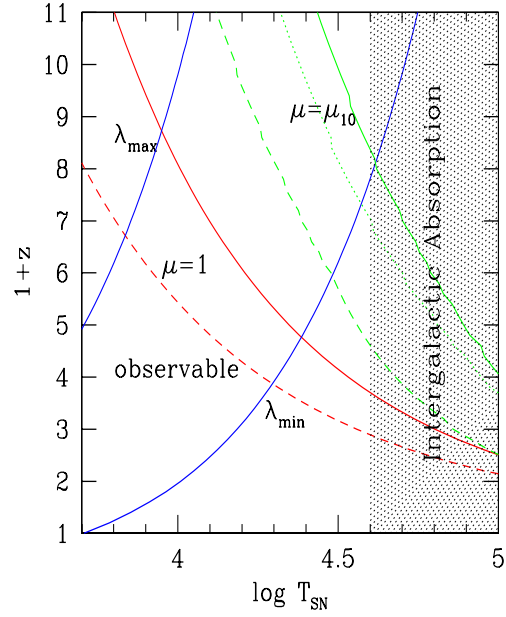


Figure 4: SN detection area (marked as "observable") in the redshift-SN temperature,  $T_{SN}$ , plane neglecting GL magnification (curves  $\mu = 1$ ) and with magnification  $\mu_{10}(z)$  for the three cosmological models: SCDM (solid curve), LCDM (dashed), CHDM (dotted). Note that for  $\mu = 1$  the SCDM and CHDM curves overlap. The area is also bound by the lower and upper NGST wavelength limits,  $\lambda_{min}$  and  $\lambda_{max}$ , respectively. The shaded region shows the effect of intergalactic absorption; the SN luminosity is  $3 \times 10^{42} \text{ erg s}^{-1}$ .

tween  $\lambda_{min}$  and  $\lambda_{max}$  with a flux larger than  $\mathcal{F}_{NGST}$ . In the absence of magnification, the upper redshift boundary of the detection area (marked as "observable" in the Figure) is  $4 < z < 8$  for  $10^4 \text{ K} \lesssim T_{SN} \lesssim 3 \times 10^4 \text{ K}$  for SCDM and CHDM models (both having  $\Omega_\Lambda = 0$ ) and  $3 < z < 5.5$  for  $8000 \text{ K} \lesssim T_{SN} \lesssim 2.5 \times 10^4 \text{ K}$  for LCDM. This difference is due to the larger luminosity distance in LCDM models. We can now compare this result with the one obtained considering the GL magnification of the SN. As an indication, we use for  $\mu$  the value of  $\mu_{10}(z)$ , *i.e.* the largest magnification with a probability  $P(\mu) > 10\%$ : this quantity should represent a good compromise between the two, usually conflicting, requirements that a high magnification and high probability event occurs. In this case, the upper redshift boundaries (the three uppermost declining curves in Fig. 4) of the detection area are shifted towards higher redshift, in a way that depends on the cosmological models, which are now clearly differentiated because of the concomitant effect of their different  $\mu_{10}(z)$  and luminosity distances. Also, the total area is generally increased, thus considerably enhancing the detection chances. The maximum redshift at which a SN can be observed is now above  $z = 10$ , the limit of our GL simulations, for all models, and it can be extrapolated to  $z \approx 12$  for SCDM. From Fig. 4, it appears that, for a SN search aimed study, the most effective improvement with respect to the planned NGST characteristics would be an extension of the bandpass into the mid-IR, which would greatly enhance

the maximum detection redshift of these objects.

### 3.3 Number Counts

Recently, Marri, Ferrara & Pozzetti (1998), have derived the expected differential number counts,  $N(m)$ , of Type II SNe in the above mentioned cosmological models, taking into account the effects of gravitational magnification. In brief, they calculate the expected SN rate per unit (co-moving) volume  $\gamma(z)$  from semi-analytical models. Next, they calculate how magnification by gravitational lensing affects the evolution of the observed SN luminosity function (LF) (assuming that the local LF is the one suggested by Van den Bergh & McClure 1994) using the following prescriptions: *i*) calculate the total number of SNe by integrating  $\gamma(z)$  in a given redshift interval  $\delta z$  around  $z_i$  and in a certain cosmic solid angle  $\omega$ ; *ii*) assign a peak luminosity to each SNe by randomly sampling the van den Bergh & McClure luminosity function; *iii*) assign to each SN a certain value of the magnification,  $\mu$ , by randomly selecting a cell of the magnification map relative to the appropriate redshift interval and cosmological model. Magnification maps and magnification probability distributions,  $P(\mu)$ , are those derived by MF.

Following MF,  $\delta z = 0.2$ ; the value of  $\omega$  is taken as the sum of 100 NGST fields, *i.e.*  $0.44 \text{ deg}^2$ ; we suppose that these fields are surveyed for one year. This experiment is well within the scheduled observational plans and capabilities of NGST (Stockman et al. 1998). Fig. 5 shows the log of the differential SNe counts as a function

of AB magnitude. The four upper panels contain the curves for the SCDM model and for  $J$ ,  $K$ ,  $L$ , and  $M$  bands, both including or neglecting the effects of gravitational lensing on the LF. The gravitational flux magnification allows the detection, at a given limiting flux, of a larger number of SNe. For comparison, we plot the NGST magnitude limit  $AB = 31.4$  (vertical line). Thus, NGST should be able to reach the peak of expected SNe count distribution, located at  $AB \approx 29 - 30$  (depending on the model), with roughly 1 mag gain brought by gravitational magnification. The three cosmological models (SCDM, LCDM, CHDM) predict a total number of (574, 2373, 164) SNe/yr in 100 surveyed fields of NGST.

From these results it appears clear that by pushing SNe searches to faint magnitudes, and exploiting the gravitational lensing magnification, we will be able to build a statistically significant sample, which will allow to test various cosmological models and study the cosmic star formation history of the universe at epochs otherwise difficult to investigate.

We are grateful to our collaborators in the project, B. Ciardi and L. Pozzetti for allowing presentation of results in advance of publication.

#### REFERENCES

- Anninos, P., & Norman, M. L. 1996, ApJ, 460, 556  
 Ciardi, B., & Ferrara, A. 1997, ApJ, 483, 5

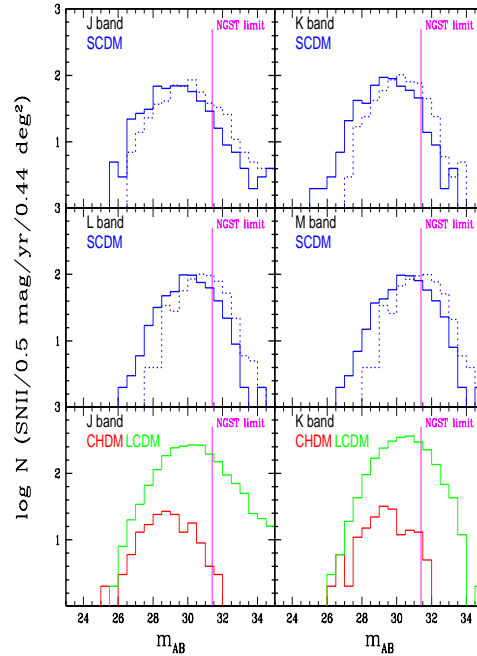


Figure 5: *Differential number counts for the three cosmological models considered as a function of apparent AB magnitude in J,K,L,M bands (LCDM and CHDM: J and K only). Also shown is the NGST limiting magnitude. Solid (dashed) curves include (neglect) lensing magnification.*



- Ciardi, B., Ferrara, A. & Abel, T. 1998, ApJ, submitted
- Carr, B. J., Bond, J. R. & Arnett, W. D. 1984, ApJ, 277, 445
- Couchman, H. M. P. & Rees, M. J. 1986, MNRAS, 221, 53
- Ferrara, A. 1998, ApJ, 499, L17
- Haiman, Z., Rees, M. J., & Loeb, A. 1997, ApJ, 476, 458
- Kashlinsky, A. & Rees, M. J. 1983, 205, 955
- Kirshner, R. P. 1990, in "Supernovae", ed. A. G. Petschek, (Springer: New York), 59
- Marri, S. & Ferrara, A. 1998, ApJ, in press (astro-ph/9806053)
- Marri, S., Ferrara, A. & Pozzetti, L. 1998, ApJ, submitted
- Ostriker, J. P. & Cowie, L. L. 1981, ApJL, 243, 127
- Palla, F., Salpeter, E. E. & Stahler, S. W. 1983, ApJ, 271, 632
- Palla, F., Galli, D. & Silk, J. 1995, ApJ, 451, 44
- Silk, J. 1977, ApJ, 211, 638
- Stockman, H. S., Stiavelli, M., Im, M., & Mather, J. C. 1998, Science with the Next Generation Space Telescope, ed. E. Smith & A. Koratkar (ASP Conf. Ser. ), in press
- Tegmark, M., Silk, J., Rees, M.J., Blanchard, A., Abel, T. & Palla, F. 1997, ApJ, 474, 1
- van den Bergh S. & McClure R. 1994, ApJ, 425, 205
- Woosley, S. E. & Weaver, T. A. 1986, ARA&A, 24, 205